Available online at www.sciencedirect.com
SCIENCE DIRECT®
Polymer 44 (2003) 6059–6066
polymer
www.elsevier.com/locate/polymer

Strength and deformation of rigid polymers: structure and topology in amorphous polymers

Z.H. Stachurski*

Department of Engineering, Faculty of Engineering and Information Technology, Australian National University, Canberra 0200, Australia

Received 20 February 2003; received in revised form 29 April 2003; accepted 12 May 2003

Dedicated to Prof. Ian M. Ward on the occasion of his 75th birthday

Abstract

Glassy polymer is formed because the irregular chain architecture prevents crystallisation. Computer simulations allow Voronoi tessellation of atomic groups (for example monomers) to be carried out and measured along the molecular chain, which reveals significant density fluctuations. A Voronoi polyhedron is constructed for each particle according to a unique mathematical procedure [J Reiner Angew Math 134 (1908) 198]. When measured in terms of Voronoi polyhedra, amorphous structures show wide variations in packing density on the atomic/monomer scale, with a characteristic skewed distribution. The Voronoi method can be applied to all polymers; however, in this paper only uncrosslinked amorphous polymers are considered. Constriction points around a chain segment are defined as a locally specific configuration and arrangement of adjacent chains such that the local density within a sphere of radius approximately equal to two monomer diameters comes close to or below the hypothetical crystalline density. The topological theory of molecular structure developed by Bader defines the concepts of atoms and bonds in terms of the topological properties of the observable charge distribution [Rep Prog Phys 44 (1981) 893]. In polymers the high density regions become an even stronger topological feature, and are referred to as the *constriction points*.

Keywords: Voronoi tessellation; Density fluctuations; Amorphous; Uncrosslinked

1. Introduction

An important point, crucial to the understanding of deformation and strength of amorphous polymers, is the concept of density fluctuations at the nano-scale dimensions. Density fluctuations have been suspected and predicted [3,4], empirically deduced [5–7], and experimentally measured [8]. X-ray scattering, with the finest beam focus, probes polymer volumes in the order of 10^8 nm^3. From that volume, the experimental measurements show a variation of approximately 2% (at 1/2 peak height) around the average body density. However, at the atomic/monomer level, density fluctuations can be an order of magnitude higher. These large fluctuations throughout the body of the polymer lead to the concept of a network of constriction points [9,10]. Then the deformation and yield strength of amorphous polymers can be viewed in terms of integrity of the network of strongest intermolecular bonds (constriction points) in a relatively weaker, lower density matrix. This is in contrast to the case of ductile metals, in which the strength of a hard matrix (crystal lattice) is determined by a network of weaknesses (dislocations).

A starting point for the description of glassy polymer structure is the concept of densely packed, entangled, random Gaussian coils, derived from the studies of polymer melts and solutions. The random coil state remains favourable in the glassy state [7,11]. Above the glass transition temperature (T_g), further structural details are provided by the Doi-Edwards theory; chains are confined to molecular tubes, within which de Gennes reptation takes place [12,13]. From NMR studies it is confirmed that the chain is not a simple (smooth), constant curvature random coil, but it is further segmented by folds (on itself) [14]. The number of folds per chain is a property of the chain (stiffness and chemistry characteristics), and of temperature ($\sim T^{1/3}$). The size of the fold is, to a good approximation, independent of temperature and chain length. The segments between the folds, of length typically between 10 and 20 covalent bonds, are considered as Rouse segments in the chain backbone [14,15]. Folds are expected to partially decouple the dynamics of the chain sections between them,

* Tel.: +61-2-6125-5681; fax: +61-2-6125-0506.
E-mail address: zbigniew.stachurski@anu.edu.au (Z.H. Stachurski).

0032-3861/03/$ - see front matter © 2003 Elsevier Ltd. All rights reserved.
doi:10.1016/S0032-3861(03)00555-X

which explains the tendency of the relaxation time (characteristic of the correlation length of the tight tube), to be independent of molecular weight. Chain segment can also be defined as a number of consecutive main chain bonds, large enough to allow conformational transition in the isolated segment when the positions of the two ends are fixed. The underlying motivation for this definition is that such a chain segment can be subjected to any general deformation. It transpires that the minimum length segment for most polymers is of the order of 10–20 covalent skeletal bonds. On cooling to below T_g, the spatial positions of the chains, with their folds and constraints, remain fixed, and unrelaxed to a large extent, obviously depending on the cooling rate. Within the macroscopic volume of the polymer, so-called 'free volume' is present as an equilibrium property of the system at $T > T_g$ [14,15]. At a sufficiently fast cooling rate from this state to a temperature below T_g the polymer retains a certain amount of the free volume. The actual amount depends on the temperature from which the quench occurs, the cooling rate, and the type of the polymer and its volume.

Glassy polymer is formed because the irregular chain architecture prevents crystallisation. On cooling to below T_g, a portion of the unoccupied free volume spontaneously diffuses out, allowing the bulk volume to reduce. In the process, the equilibrium end-to-end distance of chains is compressed. The system falls out of equilibrium, becoming trapped in a single minimum in potential energy phase space (becomes a glass) as its relaxation time rapidly increases beyond the normal experimental measuring time-scale [16]. To attain equilibrium, the glassy polymer must be able to move, with cooperatively arranged relaxations [17], between a representative subset of the minima in the potential energy surface. When held at a temperature sufficiently close to, but below T_g, the polymer structure will undergo annealing by exploring the lower energy minima not accessible during the cooling process. Thus, an annealed (or long time aged) glassy polymer can be considered to be in a static equilibrium state, but a quenched polymer may be far from equilibrium, and will exhibit structural relaxation.

This image of the glassy structure of polymers has been further enhanced, and given shape beyond the beads and links model, by visual displays of unabridged computer simulations of amorphous polymer cells, pioneered by Suter and Theodorou [18], and now available in several software packages. Amorphous polymer cells can be simulated using, for example, Materials Studio software [19]. United atom simplifications are not used. Typically, amorphous cells, with a cube edge length of approximately 3–4 nm, are formed at 50 °C below T_g, comprising several chains with a total of approximately 10^4 atoms. First, molecular chains are generated in an extended chain conformation using the polymer builder routine. Next, the amorphous cell is constructed from an initial density, typically 0.6 that of the actual density of the polymer, and minimized in size towards the target density under periodic boundary condition. Interactions between atoms include stretching, bending, rotations and out of plane distortions [20]. Short molecular dynamics (MD) runs are carried out within the same process. The roughly equilibrated structure is further minimized in approximately 5000 steps before the full MD run with approximately 10^5 steps (each step of 1 fs duration) is carried out. During equilibration the *NVT* method is used, where the number of atoms (N), volume (V) and the thermodynamic temperature (T) are held constant by coupling the system to a thermal bath, before changing to the constant volume and energy ensemble method for densification and final data collection.

Computer simulations allow Voronoi tessellation of atomic groups (for example monomers) to be carried out and measured along the molecular chain, which reveals significant density fluctuations [20,21]. The cross-sectional diameter of the chain Voronoi volume (not the same as Edwards molecular tube) varies by as much as square root of the difference between maximum to minimum density variation along its length. When described in this geometric way, the unoccupied volume is no longer treated as a 'vacancy' or 'free' volume, but rather it is associated with the space around individual atoms or atomic groups and the topology of the chains. It will change as the polymer is deformed [22–24]. At locations along the chain where the local Voronoi volume is minimal, the surrounding atoms act as constrictions on the molecular chain within, restricting motions at these locations [9,10]. The method of Voronoi tessellation, which allows precise definition of volume at the atomic level, with special application to polymers, is described below.

2. Voronoi diagrams

A Voronoi polyhedron is constructed for each particle according to a unique mathematical procedure [1,23,25]. For a set of points on a plane, each representing a particle, links are drawn between neighbouring points. Next, for each link a line is drawn perpendicular to it and passing through a point equidistant from the terminal points. Such bisectors produce polygons around the particles. For each particle, the smallest polygon so constructed is the Voronoi polygon. The sum of all Voronoi polygons is the Voronoi diagram. It is a simple matter to extend this construction to 3D with bisectors as planes instead of lines. The result is identical with the construction of the first Brillouin zone [26] (although fcc Brillouin zone gives bcc Voronoi polyhedron, and vice-versa), and similar to the geometry of grain boundaries formed under the condition of isothermal crystallisation with simultaneous random nucleation [27–29]. Thus, each particle owns a certain amount of space in the material. The partitioning of space in this way, and the formation of corresponding polyhedra is the Voronoi tessellation process; the resulting set of polyhedra

constitutes the Voronoi diagram. The shape and volume of the diagram are identical to those of the real material. This method applies equally to both crystalline and amorphous solids. In the limit of a local arrangement extending to long-range order, the Voronoi tessellation becomes identical with the Weigner-Seitz cell method for crystalline solids.

2.1. Atomic Voronoi polyhedron

A segment of hcp structure shown in Fig. 1(a) has the central atom surrounded by 12 touching atoms. In this arrangement, the surrounding atoms are in three layers: 3 + 6 + 3. Construction of Voronoi tessellation leads to a truncated hexagonal prism as shown in Fig. 1(b). The vertical faces of the hexagonal prism are created by the six atoms in the middle layer; the three atoms above and below cut off slices from the top and bottom of the prism. Similar Voronoi polyhedra for the fcc (4 + 4 + 4) and dodecahedral (1 + 5 + 5 + 1) arrangements are shown in Fig. 1(c) and (d)). In an amorphous structure formed by randomly packed spheres, an atomic Voronoi polyhedron may look like the two examples shown in Fig. 1(e) and (f). One such polyhedron will be referred to as an 'atomic Voronoi polyhedron', V_{at}. The sum of all V_{at} polyhedra is the Voronoi diagram for this material.

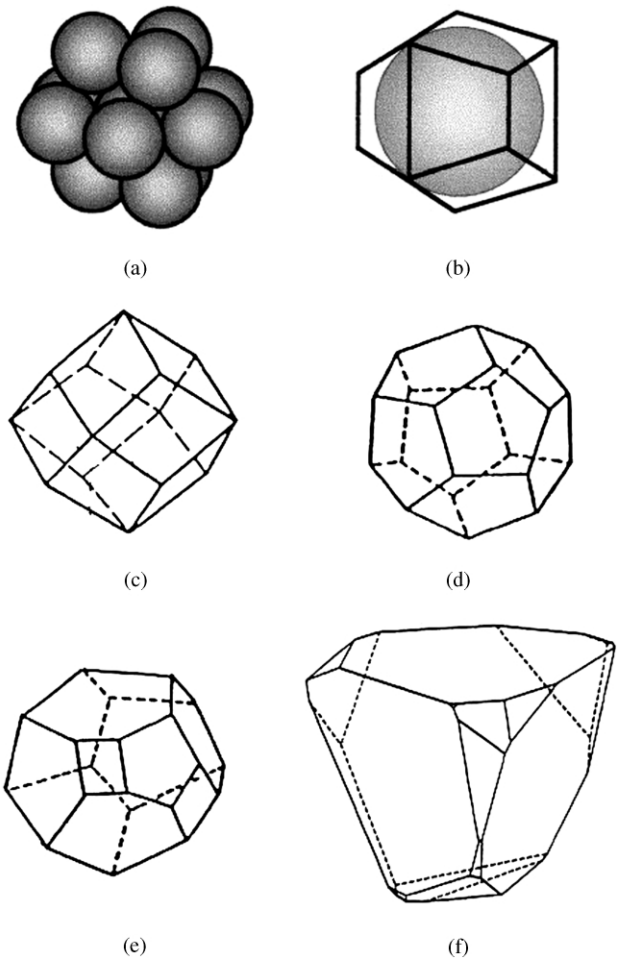

Fig. 1. Atomic (single sphere) Voronoi polyhedra: (a) hcp packing of spheres (3 + 6 + 3 touching neighbours), and (b) the corresponding Voronoi polyhedron in the shape of truncated hexagonal prism, (c) Voronoi polyhedron corresponding to fcc packing arrangement (4 + 4 + 4 touching neighbours), (d) Voronoi polyhedron corresponding to dodecahedral arrangement (1 + 5 + 5 + 1 touching neighbours); (e) and (f) examples of atomic Voronoi polyhedra for random, disordered packing, (e) with 8 touching neighbours, (f) with 6 touching neighbours.

2.2. Compound Voronoi polyhedron

For the black atom shown in Fig. 2(a) tessellation produces a polyhedron as shown in Fig. 2(b). A similar polyhedron also results for each of the white atoms since the symmetry elements of the black and white atoms are the same. The size of polyhedra depends on the distance between the atom centres, regardless of the sizes of the atoms. If adjoining atomic polyhedra (for the black and white atoms) are combined, the resultant object is a 'compound Voronoi polyhedron', V_{com}. In this case each V_{com} is associated with two atoms; its volume is equal to the volume of the crystal unit cell. The sum of all V_{com} polyhedra is the Voronoi diagram for the material.

2.3. Monomer Voronoi polyhedron

In the pseudo body-centred tetragonal crystal structure of crystalline polyethylene [30], each carbon atom has two carbon and two hydrogen atoms as closest neighbours. Voronoi tessellation results in a tetragonal polyhedron for the carbon atoms. Carrying out tessellation for each of the two hydrogen atoms and combining these with the carbon Voronoi polyhedron results in a monomer Voronoi polyhedron, V_{mon}, as shown by the heavy lines in Fig. 3(a). In this case, the volume of V_{mon} = 1/4 of the volume of the crystal unit cell. Each V_{mon} possesses the same symmetry elements as the unit cell of polyethylene.

A monomer Voronoi polyhedron for amorphous polyethylene may look like that shown in Fig. 3(b). The polyhedron will have different shape and size for each monomer. The sum of all V_{mon} polyhedra is the Voronoi diagram of the polymer.

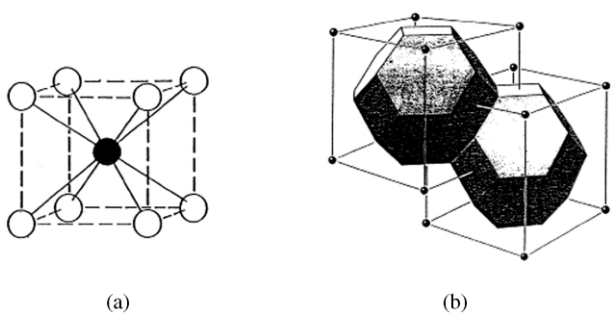

Fig. 2. Compound Voronoi polyhedron: (a) bcc packing of atoms, and (b) the corresponding Voronoi polyhedron for two atoms.

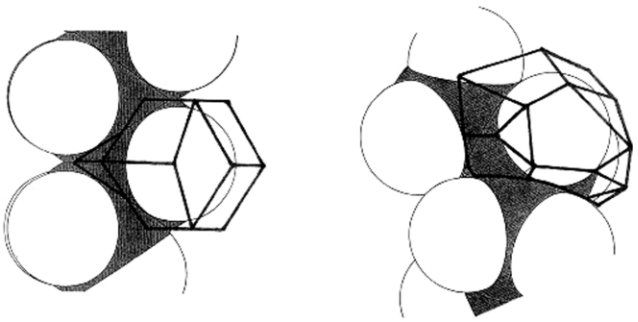

Fig. 3. Monomer Voronoi polyhedra: (a) in crystalline polyethylene, comprising one carbon and two hydrogen Voronoi polyhedra, and (b) in amorphous polyethylene.

2.4. Chain Voronoi polyhedron

Consider a hypothetical polymer chain as shown in Fig. 4. Applying the tessellation process we obtain V_{at} for each atom in the chain. If the chain contains side-groups, then through a similar process we can create the 'side-group Voronoi polyhedra', V_{sg}. By combining the appropriate adjoining polyhedra we form, V_{mon}. Continuing, we can combine the individual polyhedra according to any scheme we choose. Finally, addition of all monomer Voronoi polyhedra forms a 'chain Voronoi polyhedron', V_{cha}. The sum of all chain Voronoi polyhedra is the Voronoi diagram for the polymer.

3. Density fluctuations

When measured in terms of Voronoi polyhedra, amorphous structures show wide variations in packing density on the atomic/monomer scale, with a characteristic skewed distribution. An example of Voronoi volume (V_{at}) distribution, from a computer simulation study of random close packing of 10^5 spheres [31], is shown in Fig. 5(a). Another example of the distribution of Voronoi volumes (V_{mon}), this time from a computer simulated cell of PMMA comprising 9×10^3 atoms [20], is shown in Fig. 5(b). In the latter case atomic volumes were added to form monomer Voronoi volumes (all together 300), hence the statistics is limited and the distribution not smooth. In both cases, integration of the distributions along the horizontal axis, over the limits from minimum to maximum volumes, represents the total volume of the bodies (for which the statistics were carried out), and by definition, an integral from minimum to the average body volume, represents half the body volume.

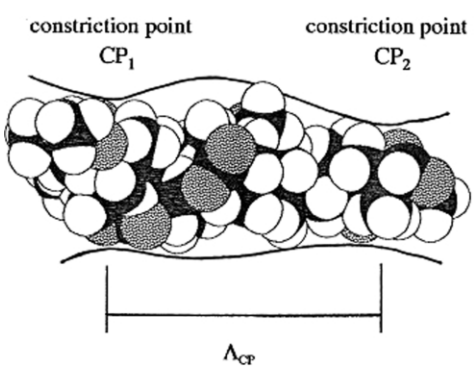

Fig. 4. A schematic drawing of the outline of chain Voronoi polyhedron around a segment of PMMA chain.

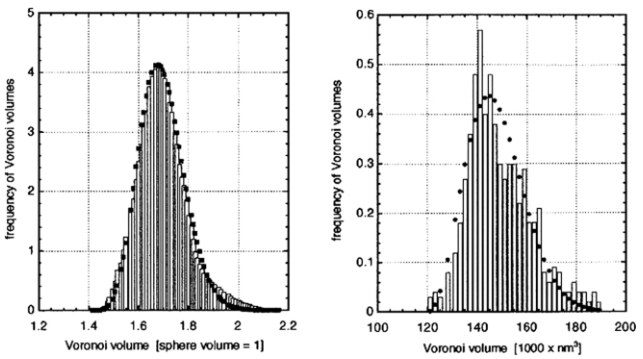

Fig. 5. Distribution of Voronoi polyhedra volumes (histogram) for two simulated systems: (a) random close packing of spheres (the smallest Voronoi polyhedron around a sphere is ~1.35 times the volume of the sphere), and (b) monomer Voronoi volumes for a cell of PMMA. The dotted curves are drawn according to Eq. (1) with $\alpha = 4.2$, and $\lambda = 0.182$ for (a), and $\alpha = 2.1$ and $\lambda = 24$ for (b).

Consider the data for the polymer cell. It is reasonable to assume that monomer Voronoi volumes with values less than that for a corresponding crystalline structure ($0.135\ nm^3$) can be considered as high density regions, whereas those with volumes above $0.160\ nm^3$ represent low density (corresponding to a state of the polymer above T_g).

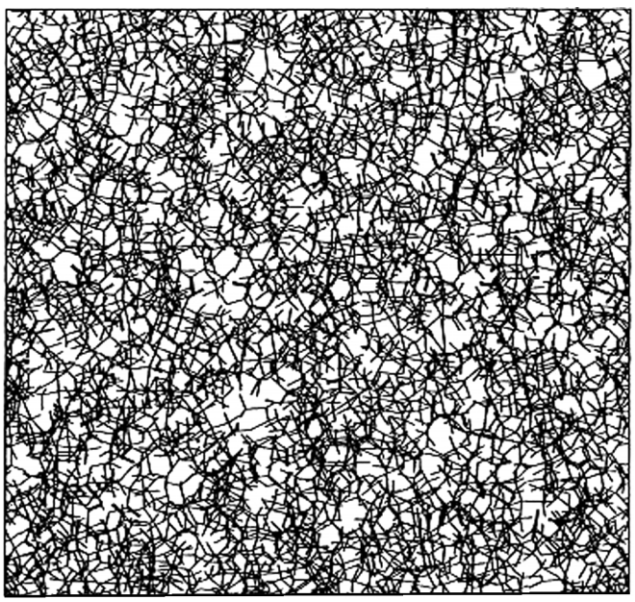

Fig. 6. View through a cube cell ($4.3 \times 4.3 \times 4.3\ nm^3$) of amorphous PMMA. The atoms have been removed, and only the bonds are visible. The projection shows significant density fluctuations.

A graphic display of these density fluctuations is shown in Fig. 6, in which the atoms have been stripped off the simulated amorphous PMMA, only the bonds showing; the view is through the thickness of the 4.3 nm cube cell. Spatial analysis of these fluctuations suggests that the structure of the polymer at nano-size dimensions can be thought of as a relatively low-density matrix in which are dispersed the high-density regions. This must not be taken strictly as a two-phase structure, since the density variation does not show discontinuities, but rather oscillates from lower to higher values periodically throughout the polymer.

4. Constriction points

Constriction point (CP) around a chain segment is defined as a locally specific configuration and arrangement of adjacent chains such that the local density within a sphere of radius approximately equal to two monomer diameters comes close to or higher than the hypothetical crystalline density (isotactic PMMA crystal has an average Voronoi volume of 0.135 nm^3, with a density of 1.12 kg/m^3, calculated using Vegard's law with tabulated data from van Krevelen [32]). Thus, a molecular chain passes through the structure, inhabiting regions of average or low density, and every so often becomes included in the CP. The V_{cha} forms a tube-like structure around the chain, widening and narrowing along its length, The chain is pinned at the narrow points by the surrounding structure, as is illustrated in Fig. 4.

The CP differs fundamentally from an entanglement. The latter exists only in polymer melts subjected to deformation and it supports dynamic tension in the chain. The former is a property of the glassy structure and its topology. In terms of molecular mechanisms of deformation, the mobility of the chain is highly limited at the CP. It is conjectured that this is a fundamental physical construction; characteristic of amorphous glassy polymers, and it determines the possible modes of deformation and yield strength, as well as chain dynamics. The collection of all CPs forms a network throughout the structure that determines the limit of anelastic recoverable deformation and ultimately its yield strength.

If we denote the number of CPs as N_ρ, then N_ρ/V is the volume average per unit volume, and N_ρ/N is the number average per monomer. If Voronoi tessellation of a cell of volume V, results in a distribution $\Phi(V_V)$, then the fraction of CPs in the structure is measured by the fractional area under the Voronoi volume distribution peak, measured from the minimum volume to the crystalline (density) volume (Fig. 5(b)). From the description given above one can infer that the number of CPs (in a given glassy polymer) will be a function of the cooling rate and melt temperature, as well as the possible structural relaxation due to ageing or annealing.

5. Discussion and conclusions

The complete development of plasticity theory in crystalline solids depended on the coexistence of three essential elements of knowledge:

1. Theory of crystallography providing precise definition of ideal crystalline solids (Stensen—1680, Haüy—1780, Miller—1860, Bravais—1890, Bragg—1920, etc.),
2. Mechanisms of plastic deformation (Taylor—1938 edge dislocation, Frank and Reid—1952 screw dislocation, Tammann—1958 shear transformation),
3. Experimental method(s) of verification (electron microscopy—1948; supplementary: single crystal deformation morphology, etch pits microscopy, X-ray tomography, and other).

The above three elements are also necessary and essential for a complete understanding of deformation and plasticity in amorphous polymers. Thus, a method equivalent to electron microscopy is effectively provided by computer simulations and nuclear magnetic resonance of amorphous polymers [33–35]. Many theories of mechanisms of plastic deformation in polymers exist in published literature, and have been reviewed [36–38]. However, the first essential element, namely a theory of the structure of amorphous solid polymers, is not developed yet in sufficient detail (in comparison to the theory of crystallography) to afford the clarity of understanding required to describe precisely individual molecular motions, and the accompanying changes in nano-structure during plastic deformation occurring in amorphous polymers. It is frequently tacitly assumed that amorphous materials are found at the limits of disorder, and especially for polymers, amorphicity is usually defined by what *it is not*, rather than by what it is, hence many approaches to plasticity in amorphous polymers were based on concepts derived from dislocation theory.

In the range of temperatures: $\sim (2/3)T_g < T < T_g$, many amorphous polymers show ductile behaviour (if crazing and fracture is prevented), similar to the ductile deformation of metals at high temperatures, i.e. $\sim 0.6T_m < T < T_m$, in which flow stress is governed by lattice self-diffusion mechanisms. As a result of rapid self-diffusion, dislocations re-arrange into a sub-grain network, which becomes the most important structural parameter. In amorphous polymers the concept of a dislocation is inappropriate [39], and self-diffusion by reptation (in uncrosslinked polymers), even at the relatively high temperatures, is a slow process. Amorphous crosslinked polymers also show yield behaviour below T_g [40,41]. However, the variety and complexity of their network structures requires careful description and analysis before a plausible physical mechanism of yield can be proposed [40]. Most importantly, the structure at the nano-scale level is far more inhomogeneous in amorphous polymers than that found in pure polycrystalline materials.

An insight into density fluctuations in amorphous

structures can be gained by considering an earlier developed model of random dense packing of N hard spheres of identical diameter, a, which are to a large extent in contact [42,43]. Let the body, of numerical density, $\rho_b = N/V$, be divided into smaller pieces, and the pieces divided into smaller pieces. For many subsequent divisions the density of each piece will be the same. Eventually, there will be a piece of the smallest representative volume element for which the density is still the same and equal to ρ_b (this translational invariance in the mean is a requirement imposed on all macroscopically large disordered systems [39,44]). By implication, a further division into volumes smaller than the representative volume element will result in deviations of density. Therefore, ρ_b is an average density of the body: $\rho_b = \bar{\rho}$. In the limit, the largest variations in local densities, ρ_i, are found when volumes around each sphere are expressed in terms of corresponding Voronoi polyhedra. Noting that, for random densely packed spheres of same size the average density, expressed in terms of packing fraction, is approximately 0.64 [45], and that the maximum is 0.74 for ordered close packed structure, the following firm observations can be made: (i) for a symmetric distribution around the above average value the following is true $|\rho(\min) - \bar{\rho}| = |\rho(\max) - \bar{\rho}|$, providing a value for the minimum density, $\rho(\min) = 0.54$. The maximum width of density fluctuation in this case is: $2[\rho(\max) - \bar{\rho}]/\bar{\rho} \cong 0.31$. (ii) For a non-symmetric distribution the minimum value of density (for any sphere inside the body) must be finite and greater than zero. The width of local density fluctuations in this case must be even greater than 0.31.

The conclusion can be drawn that, even in the simplest of all systems (uniform spheres), wide density fluctuations at the atomic level are consequent on random packing. Non-symmetrical density fluctuations are to be expected, reflecting the limited availability of space at the $\rho(\max)$-end. Voronoi volume distributions, which are simply related to density distributions, have been studied for a whole variety of packings, and the non-symmetric shape appears to be ubiquitous in published literature [43,46–48], and also evident in Fig. 5. Therefore, in amorphous polymers, non-symmetric wide density fluctuations are inevitable and observable, although symmetric distributions have been suggested [8]. It is well known that density fluctuations causing losses in optical fibres made from silica glass are of the order of 10^{-4}, as shown by experiments using radiation with a wavelength of several μm. With X-ray radiation the wavelength is very short, but the irradiated volume is still large, yielding calculated density fluctuations of the order of 2×10^{-2}. It is reasonable to make the conjecture that scattering experiments on glassy polymers with radiation of wavelength approximately 1 nm should reveal the large density fluctuations of the order of 10^{-1} as predicted from the distribution of Voronoi volumes.

An attempt at the analysis of the shape of the distribution has been published [48]. For the purpose of describing it with a continuous curve, a simple empirical function has been chosen as follows:

$$\Phi(V_V) = x^{\alpha} \exp(-(x/\lambda)^2), \qquad x = (V_V - V_0) \tag{1}$$

where V_V is the Voronoi volume for an atom, (or monomer), V_0 is the corresponding minimum volume extrapolated to 0 K, λ describes the width of the peak, and is related to the average volume, $\bar{V}$. The exponent, α, and the constant, λ, are chosen to fit to a given distribution. A fit to the discrete distribution in Fig. 5(a) is obtained with the following values: $\alpha = 4.2$ and $\lambda = 0.182$, and for Fig. 5(b): $\alpha = 2.1$ and $\lambda = 24$.

All Voronoi polyhedra obey the Euler relationship [49]:

$$V - E + F = 2 \tag{2}$$

where V, E and F represent the number of vertices, edges and faces of a polyhedron, respectively. The Voronoi polyhedron with a minimum number of faces is a tetrahedron. In general, Voronoi polyhedra contain many faces as seen in Figs. 1–4; some faces contain touching contact points between atoms (as a rule on the largest polyhedron faces [25,27,50]). The largest number of contact points per Voronoi polyhedron for equal sized spheres is 12 (fcc, hcp or icosahedron arrangements). From the geometry of construction of atomic Voronoi polyhedra it follows that they are convex [25,49], whereas all group Voronoi polyhedra, including compound, monomer and chain, are in general both convex and concave, as shown in this paper. And lastly, it can be noted that for pure and ideal crystalline substances, all Voronoi polyhedra are precisely of the same size and shape for the same type of atoms (equivalent to Weigner-Seitz cells), whereas for amorphous structures Voronoi polyhedra vary in size and shape, and the distribution of Voronoi volumes is bound within limits, as is evident from the discussion above.

In crystalline solids subject to infinitesimal homogeneous elastic deformation, there is no change in the number of faces, edges and vertices of the Voronoi polyhedra [24]. It is hypothesised that in amorphous solids subject to infinitesimal homogeneous elastic deformation, the deformation of Voronoi polyhedra differs from atom to atom and monomer-to-monomer, however there will be no change in the number of faces, edges and vertices. In both crystalline and amorphous solids subject to anelastic and plastic flow deformation, Voronoi polyhedra undergo metamorphosis resulting in a change of shape, size, and a change in the number of faces, edges and vertices [24].

In solids we rely on the Born-Oppenheimer approximation [26] to decouple the motions of electrons from that of the nuclei, resulting in the concept of a stationary potential energy surface. The topological theory of molecular structure developed by Bader [2] defines the concepts of atoms and bonds in terms of the topological properties of the observable charge distribution. This provides a tentative basis for a linking relationship between quantum mechanics of the molecular structure and its geometrical description in terms of Voronoi polyhedra.

According to Bader, given a potential energy surface, the variations of its topology are expressed in terms of a weak function of the form [39,44,51]:

$$\hat{T}_\delta E(s_o, X) \approx E(s_o, X + \delta) \tag{3}$$

where $\hat{T}_\delta$ is a translational operator, δ is an arbitrary variable vector, $E(s_o)$ describes the static potential energy surface, with $s_o(x, X)$ as a parameter describing the equilibrium state, and x and X as the coordinates of the electrons and nuclei, respectively. Following the approach by Mezey [52], one can partition the nuclear configuration space into *catchment regions* determined by the gradient vector field:

$$\Delta\vec{E} = -\nabla x E(s_o) \tag{4}$$

Mezey defined topologically the catchment region as an energetically stable geometry of the open region of $\mathbf{R}^3$ traversed by all the trajectories defined by Eq. (4), which terminate at a local maximum in $-E(s_o)$. The boundaries of a catchment region are the surfaces of zero flux in the vector defined by Eq. (4). The boundaries of the catchment region have a close geometrical correspondence with the Voronoi polyhedron for a given atom/atomic group in a given structure. A catchment region is a region with local density, $\rho_i \gg \bar{\rho}$.. In an amorphous polymer, it will be made up of a cluster of small sized V_{mon} polyhedra, surrounded by medium and larger size Voronoi polyhedra. Such regions can be defined by a function similar to Eq. (3), with the stronger requirement:

$$\hat{T}_R E(s_o, r) \cong \hat{T}_R E(s_o, r + R), \text{ for } \hat{T}_R < R \tag{5}$$

where $\hat{T}_R$ is a translational operator, R is a characteristic vector of magnitude larger than the diameter of a polymer chain, and the atomic position variable, X, has been replaced by the position variable of the monomer centres, r. The exact value of R, and therefore, the number of densely packed monomers included will be determined by our notion of a high density region, which may depend on the chosen experimental measuring technique, or the specific property under consideration that depends on such quantities. The high-density regions become an even stronger topological feature, and are referred to as the *constriction points* (CPs). Clearly, the vector R, is a structural parameter, and it can be identified with the average spacing between the constriction points, Λ_{CP} (Fig. 4), and therefore characteristic of the topological features of the amorphous polymer.

In conclusion, the Voronoi tessellation method is a useful tool for geometrical description of the structure of amorphous polymers from sub-nano to macro-scale levels [53]. The width of the monomer Voronoi volume distribution is a measure of amorphicity, and the details of fine structure can be derived by considering individual atomic polyhedra. The obvious limitation of the method is that it can only be applied to objects existing within the virtual space created by a computer. Analysis of such virtual amorphous cells reveals large periodic density fluctuations, which in (uncrosslinked) polymers leads to (and provides evidence for) the concept of constriction points. Finally, the relationship between the topological features of the potential energy surface and the local disposition of Voronoi polyhedra is indicated by drawing analogy between the catchment regions and the constriction points.

References

[1] Voronoi G. J Reiner Angew Math 1908;134:198.
[2] Bader RFW, Nguyen-Dang TT, Tal Y. Rep Prog Phys 1981;44:893.
[3] Eyring H. J Chem Phys 1936;4:283.
[4] Bueche F. J Chem Phys 1956;24:418.
[5] Adam G, Gibbs JH. J Chem Phys 1965;43:139.
[6] Ferry JD, Williams ML, Fitzgerald ER. J Phys Chem 1955;59:403.
[7] Flory PJ. J Macromol Sci 1976;B12:1.
[8] Floudas G, Pakula T, Stamm M, Fischer EW. Macromolecules 1993; 26:1671.
[9] Stachurski ZH. J Mater Sci 1986;21:3231.
[10] Edwards SF, Vilgis Th. Polymer 1987;28:375.
[11] Birshtein TM, Sariban AA, Skvortsov AM. Polymer 1982;23:1481.
[12] de Gennes P-G. Macromolecules 1976;9:594.
[13] Doi M, Edwards SF. J Chem Soc Faraday Trans II 1978;74:918.
[14] Kimmich R, Köpf M. Prog Coll Polym Sci 1989;80:8.
[15] Inoue T, Osaki K. Macromolecules 1995;29:1595.
[16] Angell CA. J Res NIST 1991;1.
[17] Gómez Ribelles JL, Garayo AV, Gowie JMG, Ferguson R, Harris S, McEwen IJ. Polymer 1998;40:183.
[18] Theodorou DN, Suter UW. Macromolecules 1985;18:1467.
[19] Accelrys Inc, San Francisco, USA, or Cambridge Molecular Simulations Inc, Massachusetts, USA, and others.
[20] Pfister LA, Stachurski ZH. Polymer 2002;43:7419.
[21] Lousteau B. Private communication. ETH-Z, Zürich, Switzerland: Institute for Polymers; 1998.
[22] Theodorou DN, Suter UW. Macromolecules 1986;19:379.
[23] Hutnik M, Argon AS, Suter UW. Macromolecules 1991;24:5970.
[24] Stachurski ZH, Brostow W. Polimery 2001;46(5):302.
[25] Brostow W, Dussault J-P, Fox BL. J Comput Phys 1978;29(1):81.
[26] Kittel Ch. Solid state physics. New York: Wiley; 1976.
[27] Meijering JL. Philips Res Rep 1953;8:270.
[28] Piórkowska E, Galenski A. J Polym Sci Phys 1985;23:1723.
[29] Stachurski ZH, Macnicol J. Polymer 1998;39:5717.
[30] Keller A. J Polym Sci 1955;17:351.
[31] To L, Stachurski Z.H. J non-cryst solids Submitted for publication.
[32] van Krevelen DW, Hoftyzer PJ. Properties of polymers, their estimation and correlation with chemical structure. Amsterdam, New York: Elsevier; 1976.
[33] Maxwell AS, Ward IM, Laupretre F, Monnerie L. Polymer 1998;39: 6835.
[34] Theodorou D, Suter UW. Macromolecules 1986;19:139.
[35] Villain J, Szeto KY, Minchau B, Renz W. Computer simulation studies in condensed matter physics III. In: Landau DP, Mon KK, Schütelr H-B, editors. Heidelberg: Springer; 1991.
[36] Duckett RA. Int Metals Rev 1983;28:158.
[37] G'Sell C. Strength of metals and alloys. In: McQueen HJ, Bailon J-P, Dickson JI, Jonas JJ, Akben MG, editors. Proceedings of ICSMA 7, vol. 3. Oxford: Pergamon Press; 1985. p. 1943.
[38] Stachurski ZH. Prog Polym Sci 1993;22:104.
[39] Ziman JM. Models of disorder. Cambridge: Cambridge University Press; 1979.
[40] Fischer M. Adv Polym Sci 1992;100:313.
[41] Scherzer T. J Appl Polym Sci 1995;58:501.
[42] Bernal JD. Proc Roy Soc (London) 1964;194:957.
[43] Finney JL. Proc Roy Soc 1970;A319:479.

[44] Lifshitz IM, Gredeskul SA, Pastur LA. Introduction to the theory of disordered systems. New York: Wiley; 1988.
[45] Torquato S, Truskett TM, Debenedetti PG. Phys Rev Lett 2000;84:2064.
[46] Tsumuraya K, Ishibashi K, Kusunoki K. Phys Rev 1993;B47:8552.
[47] Reiss H, Hammerich AD. J Chem Phys 1986;90:6252.
[48] Hanson HG. J Stat Phys 1983;30(3):591.
[49] Miles RE. Suppl Adv Appl Prob 1972;243.
[50] Queen MP, Watson DF. J Appl Prob 1984;21:548.
[51] Stoyan D, Kendall WS, Mecke J. Stochastic geometry and its applications. Chichester: Wiley; 1987.
[52] Mezey PG. Theor Chim Acta 1981;58:309.
[53] Voronoi tessellation routine is standard with MatLab 6.5 (The Mathworks Inc.), as well as with Materials Studio [51], and other software.